CANADA

DEPARTMENT OF
ENERGY, MINES AND RESOURCES
MINES BRANCH
OTTAWA

GLASS INSERT STRESSMETERS

K. BARRON

FUELS AND MINING PRACTICE DIVISION

Reprinted from Society of Mining Engineers
December 1965

Reprint Series RS 15

Price 25 cents

Available by mail from the Queen's Printer, Ottawa,
and at the following Canadian Government bookshops:

OTTAWA
Daly Building, Corner Mackenzie and Rideau

TORONTO
Mackenzie Building, 36 Adelaide St. East

MONTREAL
Aeterna-Vie Building, 1182 St. Catherine St. West

or through your bookseller

A deposit copy of this publication is also available
for reference in public libraries across Canada

Price 25 cents Cat. No. M38-8/15

Price subject to change without notice

ROGER DUHAMEL, F.R.S.C.
Queen's Printer and Controller of Stationery
Ottawa, Canada
1966

GLASS INSERT STRESSMETERS

by K. Barron

The glass insert stressmeter, or photoelastic stressmeter, is an instrument designed to determine stress changes occurring in rocks. It has several potential advantages over other such devices in that it is a biaxial device, it is simple and it is cheap to make.

The object of this study was to assess the behaviour of the meter under biaxial loads and to examine some of the problems associated with measurement and interpretation of the fringe pattern. This assessment has been carried out by comparing theoretical and laboratory behaviour of the meter.

It has been shown that:

a) There are certain optimum measuring points in the meter at which measurements should be made for best accuracy. The position of the points depends on the ratio, η, of the biaxial stresses.

b) The meter's sensitivity can be assumed to be independent of the rock modulus E provided that the rock modulus is $< 2.5 \times 10^6$ psi and not, as previous workers have assumed, if $E < 5 \times 10^6$ psi.

c) There are several methods of separating the principal stresses; some of these are unsatisfactory. A new method is proposed and discussed.

d) The meter sensitivity decreases as the ratio of the biaxial stresses approaches unity; the accuracy thus also decreases.

e) The axes of symmetry of the fringe pattern give an excellent indication of applied stress direction.

f) Laboratory calibrations are in good agreement with theory.

The glass insert or photoelastic stressmeter is an instrument designed to determine stress changes occurring in rocks. It has several potential advantages over other such devices in that it is a biaxial device, it is simple and it is cheap to make.

This stressmeter has been described in detail.[1,2] Basically it is a hollow glass cylinder that has at one end a light source and filters producing circularly polarized light. The glass cylinder and source are grouted into a borehole in rock and the face of the cylinder is viewed through a quarter wave plate and an analyser. If, after installation, a stress change occurs in the rock, then a distinct colored isochromatic fringe pattern is seen in the meter. The fringe order at any point in the meter can be determined by counting the fringes and measuring the fractional fringe orders by the Tardy compensation method.[3] The relation between the fringe order at any point and the applied stress change can be determined either by calculation or by calibration.

The object of this study was to assess the behavior of this stressmeter under biaxial loading conditions and to examine some of the problems of interpretation of the fringe pattern.

THEORY

Hiramatsu et al[4] have determined the stress distribution in a hollow cylindrical inclusion in an elastic host material when subject to uniaxial stress. Using this solution, the biaxial case of stress p in the x direction and stress q in the y direction (Fig. 1) can be solved by superposition. This has been done in Appendix 1. It is shown that the principal stress difference $(\sigma_1 - \sigma_2)$ at any point (r, θ) in the cylinder is given by:

$$(\sigma_1 - \sigma_2) = \{[k_1(p+q) - k_2(p-q)\cos 2\theta]^2 + k_3^2(p-q)^2 \sin^2 2\theta\}^{1/2} \quad [1]$$

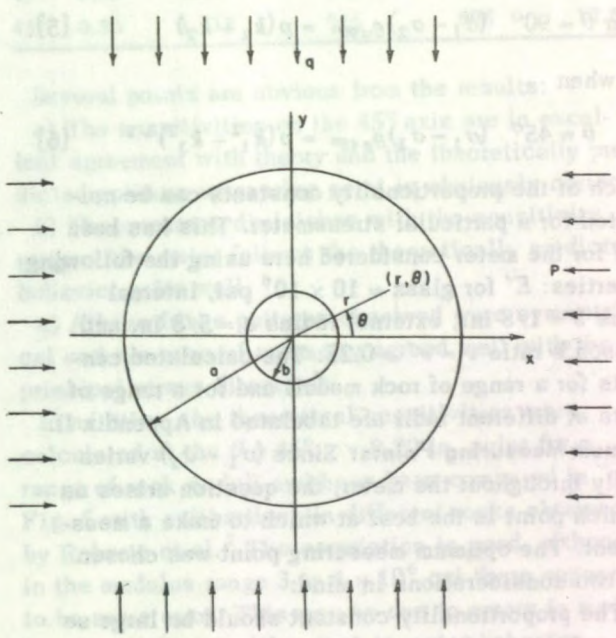

Fig. 1 – Cross section through the meter.

K. BARRON is Senior Scientific Officer, Mining Research Laboratories, Fuels and Mining Practice Div., Mines Branch, Department of Mines and Technical Surveys, Ottawa, Canada. TP 65AM19. Manuscript, Nov. 2, 1964. Chicago Meeting, February 1965. Discussion of this paper, submitted in duplicate prior to Mar. 15, 1966, will appear in SME Transactions, June 1966, and AIME Transactions, 1966, vol. 235.

where k_1, k_2 and k_3 are constants that are dependent on the dimensions and properties of the rock and the inclusion and are defined in Appendix 1.

The principal stress difference at a point is directly proportional to the isochromatic fringe order, n, observed at that point and is given by:

$$n = (\sigma_1 - \sigma_2)\frac{t}{f} \qquad [2]$$

where t is the cylinder length and f is the optical constant of the glass.

Thus Eq. 1 and 2 define the fringe order at any point in the meter in terms of the biaxial stresses p and q in the rock, i.e., they define the use of the cylinder as a stress sensing device.

An additional important point resulting from the theory is that the orientation of the principal stresses in the plane of the meter is given by the axes of symmetry of the fringe pattern in the meter.

GLASS INSERT STRESSMETERS UNDER UNIAXIAL LOADS

Theory: For uniaxial applied stress Eq. 1 becomes:

$$(\sigma_1 - \sigma_2) = p\{[k_1 - k_2 \cos 2\theta]^2 + k_3^2 \sin^2 2\theta\}^{1/2} \qquad [3]$$

In this case the fringe order is directly proportional to the stress change, p, in the rock. Hence, if the constant of proportionality is known, then a measure of the fringe order enables p to be determined.

Consider the possibilities of making measurements on each of the three axes defined by $\theta = 0°$ (x axis), $\theta = 90°$ (y axis) and $\theta = 45°$. In each case Eq. 3 is further simplified.

When $\theta = 0°$ $\quad (\sigma_1 - \sigma_2)_{\theta=0°} = p(k_1 - k_2)$ [4]

when $\theta = 90°$ $\quad (\sigma_1 - \sigma_2)_{\theta=90°} = p(k_1 + k_2)$ [5]

and when

$$\theta = 45° \quad (\sigma_1 - \sigma_2)_{\theta=45°} = p(k_1^2 + k_3^2)^{1/2} \qquad [6]$$

Each of the proportionality constants can be calculated for a particular stressmeter. This has been done for the meter considered here using the following properties: E' for glass = 10×10^6 psi, internal radius $b = 1/8$ in., external radius $a = 5/8$ in. and Poisson's ratio $\nu = \nu' = 0.25$. The calculated constants for a range of rock moduli and for a range of points at different radii are tabulated in Appendix II.

Optimum Measuring Points: Since $(\sigma_1 - \sigma_2)$ varies rapidly throughout the meter, the question arises as to which point is the best at which to make a measurement. The optimum measuring point was chosen with two considerations in mind:

a) The proportionality constant should be large so that a maximum change in fringe order is observed for a minimum stress change, i.e. good sensitivity.

b) The change of $(\sigma_1 - \sigma_2)$ with radial position should be small so that errors in defining radius during measurement do not cause large changes in constants and hence in the fringe order determined, i.e. good accuracy.

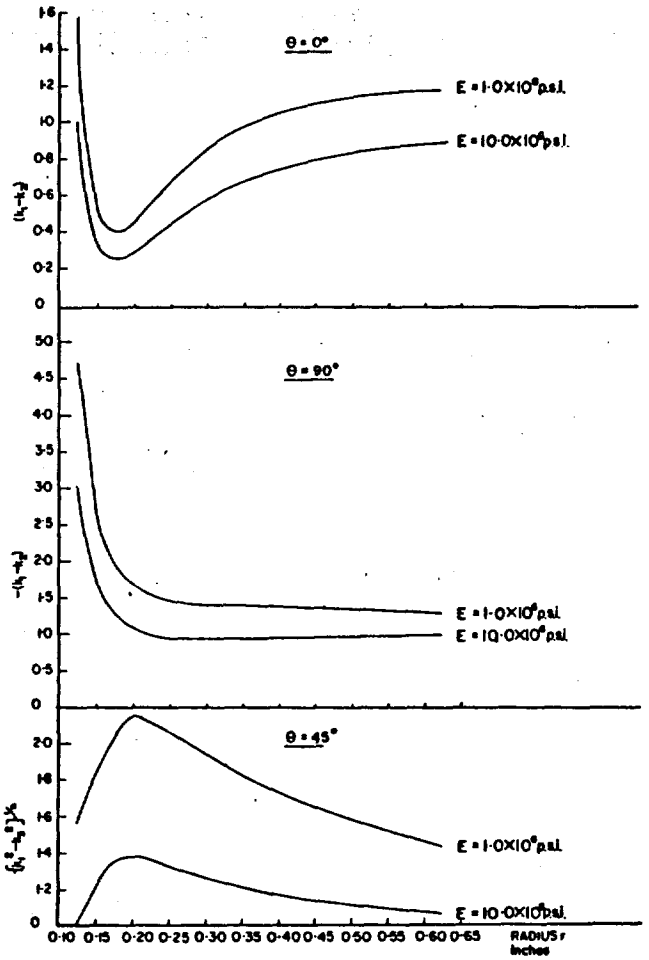

Fig. 2 — Variation of proportionality constants on $\theta = 0°$, $90°$ and $45°$ axes — uniaxial loads.

Using the calculated constants, Fig. 2 was drawn showing the variation of the proportionality constants on each of the three axes with radius for a range of rock modulus. Examination of these graphs for compatibility of the above two requirements enables the best measuring point on each axis to be selected and, by comparison, the optimum measuring point in the meter to be determined.

On the $\theta = 0°$ axis the best point is in the region $r > 0.35$ in. On the $\theta = 90°$ axis the best point is in the region $r > 0.30$ in. On the $\theta = 45°$ axis the best point is at a radius $r = 0.20$ in. Comparison of each of the three axes shows that the optimum measuring point in the meter is at $r = 0.20$ in., $\theta = 45°$. This does not necessarily apply if the applied stress is other than uniaxial.

Dependency on Rock Modulus: The meter sensitivity at any point varies with the elastic modulus, E, of the rock. It has been assumed previously [1,2] that the meter behaves similarly to a solid inclusion and,

therefore, that Coutinho's conclusions[5] apply, i.e., that the meter sensitivity is relatively unaffected by rock modulus when the inclusion modulus is greater than twice that of the rock. This assumption is not strictly true since a central hole has been introduced in the inclusion.

Consider the optimum measuring point, $r = 0.20$ in., $\theta = 45°$. Fig. 3 shows the variation of the proportionality constant at this point with rock modulus. It is seen that a change of rock modulus from 5×10^6 psi to 1×10^6 psi produces a change in proportionality constant from 1.7 to 2.15; i.e., if Coutinho's conclusions are applied to the hollow inclusion an error greater than 20% results (cf. 10% for a solid inclusion). This is a significant error. On the other hand, if the criterion is modified so that modulus ratio $E'/E > 4$ is considered, then a tolerable error of less than 10% is introduced. Thus the sensitivity of the glass stressmeter is relatively unaffected by rock modulus when the inclusion's modulus is greater than four times that of the rock, i.e., for the glass stressmeter if the rock modulus, $E \leq 2.5 \times 10^6$ psi.

It should be made quite clear that this does not prohibit the use of the meter in rocks of modulus greater than 2.5×10^6 psi, but in this case the rock modulus must be known.

Laboratory Calibration: As the meter has no moving parts, it was thought that a fair assessment of the meter behavior could be obtained from comparison of actual calibrations with those theoretically predicted. A glass stressmeter, 1-1/2 in. long, was grouted into an aluminium block ($E = 10 \times 10^6$ psi) and subjected to known uniaxial stress changes. Fringe orders were measured with incremental loads at different radii on each of the $\theta = 0°$, 45° and 90° axes. Fig. 4 shows some of these calibrations and Table I below compares the theoretical and calibration sensitivities. The theoretical sensitivities were calculated using a value for the optical constant of glass of 1030 psi per fringe per in.

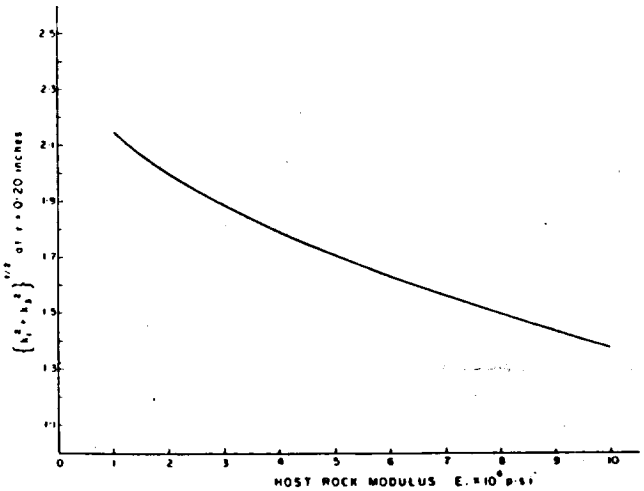

Fig. 3 — Variation of proportionality constant at optimum point with rock modulus.

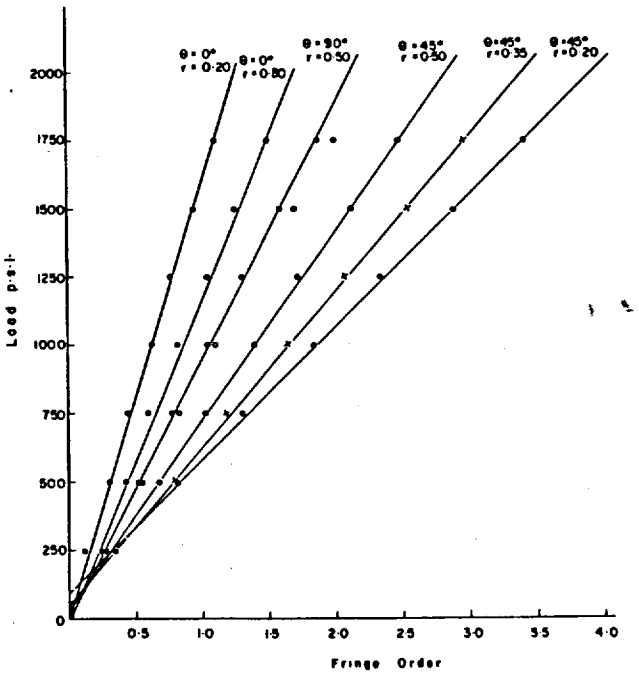

Fig. 4 — Uniaxial calibrations.

Table I. Uniaxial Sensitivities

θ	r	Proportionality Constant	p/n Theory psi/fringe	p/n Calibr psi/fringe	% Difference From Theory
0°	0.20	0.29	2370	1590	33.2
0°	0.35	0.67	1070	1240	21.0
0°	0.50	0.87	840	1175	40.0
90°	0.20	1.07	642	720	10.8
90°	0.35	0.92	748	870	16.3
90°	0.50	0.95	725	930	28.6
45°	0.20	1.38	498	484	2.8
45°	0.35	1.21	568	570	0.4
45°	0.50	1.115	616	695	12.8

Several points are obvious from the results:

a) The sensitivities on the 45° axis are in excellent agreement with theory and the theoretically predicted optimum measuring point is obviously correct.

b) The accuracy diminishes with the sensitivity. In general the meter follows the theoretically predicted behavior quite well.

c) All the fringe patterns observed were symmetrical and the axes of symmetry agreed well with the principal stress directions.

In addition, the theoretical sensitivities were calculated at the $\theta = 45°$, $r = 0.20$ in. point for a range of rock moduli and have been compared in Fig. 5 with calibrations in different rocks obtained by Roberts et al.[2] The correlation is good, although in the modulus range 3 to 4×10^6 psi there appears to be some error. This may be due to errors in modulus determination rather than to meter behavior.

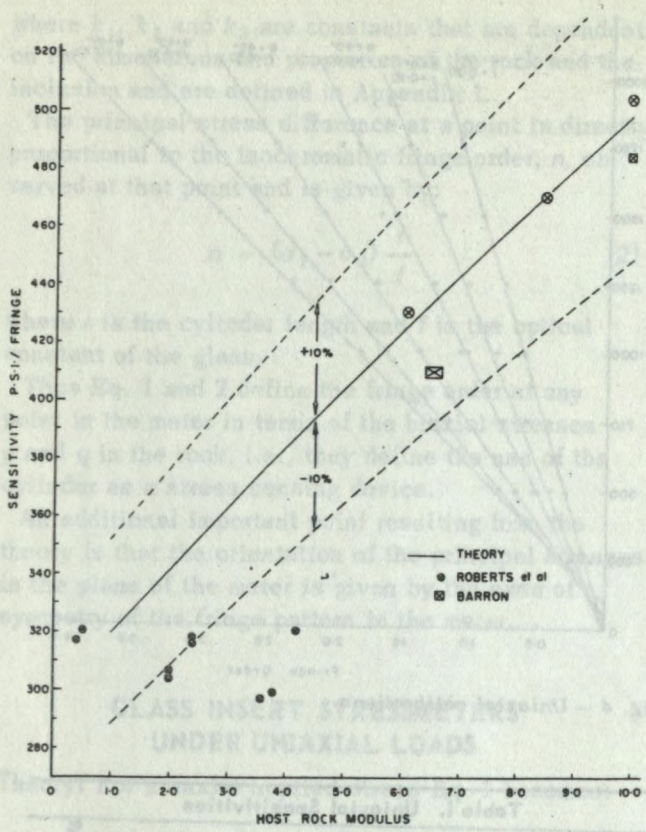

Fig. 5 – Sensitivity variation with rock modulus – uniaxial loading.

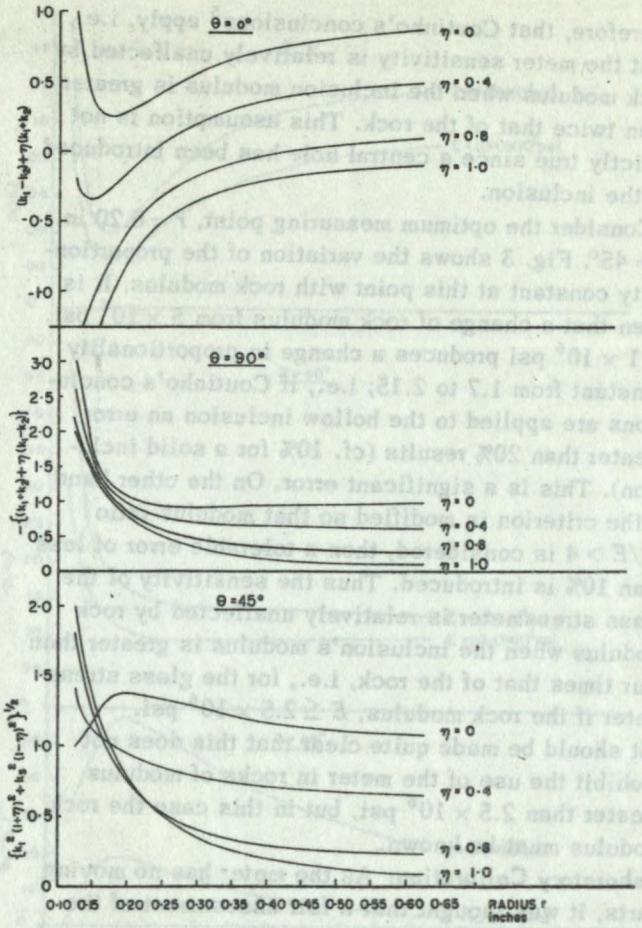

Fig. 6 – Variation of proportionality constants on $\theta = 0°$, 90° and 45° axes – biaxial loads.

GLASS INSERT STRESSMETERS UNDER BIAXIAL LOADS

Theory: Eq. 1 and 2 define the fringe order at any point when the meter is subjected to biaxial stresses. On the $\theta = 0°$, 90° and 45° axes these equations simplify to give:

When $\theta = 0°$,

$$n_x = \frac{pt}{f}\{(k_1 - k_2) + \eta(k_1 + k_2)\} \quad [7]$$

when $\theta = 90°$,

$$n_y = \frac{pt}{f}\{(k_1 + k_2) + \eta(k_1 - k_2)\} \quad [8]$$

and when $\theta = 45°$,

$$n_{xy} = \frac{pt}{f}\{k_1^2(1+\eta)^2 + k_3^2(1-\eta)^2\}^{1/2} \quad [9]$$

where n_x, n_y, n_{xy}, are the fringe orders on the 0°, 90° and 45° axes respectively and η is the ratio q/p. Fig. 6 shows the variation of the proportionality constants in the above equations with radius for a rock modulus of 10×10^6 psi and a range of η from 0 to 1.

Separation of the Biaxial Stresses *p* and *q*: Several methods have been proposed to separate p and q in Eq. 7, 8 and 9. These are discussed below.

MEASUREMENTS AT TWO POINTS – If two measurements are made at the same radius, one on the $\theta = 0°$ axis and one on the $\theta = 90°$ axis then it can be shown from Eq. 7 and 8 that:

$$p = \frac{f}{4tk_1k_2}\{k_2(n_x + n_y) + k_1(n_y - n_x)\} \quad [10]$$

and

$$q = \frac{f}{4tk_1k_2}\{k_2(n_x + n_y) - k_1(n_y - n_x)\} \quad [11]$$

Fig. 6 indicates how n_x and n_y vary with radius for different ratios η. Since it is difficult to make an exact fringe order measurement when the magnitude of fringe order changes rapidly with radius, measurements are restricted to the region $r > 0.30$ in. Now in this region the magnitude of the fringe order observed decreases considerably as η increases from 0 to 1. Thus under biaxial stresses the fringe orders will be relatively small and the measurement error correspondingly larger. Further, to separate p and q it is necessary to take the difference $(n_y - n_x)$; hence any error will be compounded. Thus, except under high stresses, the method does not appear to be practical.

Hiramatsu[6] suggests this method, but recommends the use of a Babinet compensator to determine fractional fringe orders rather than by goniometric com-

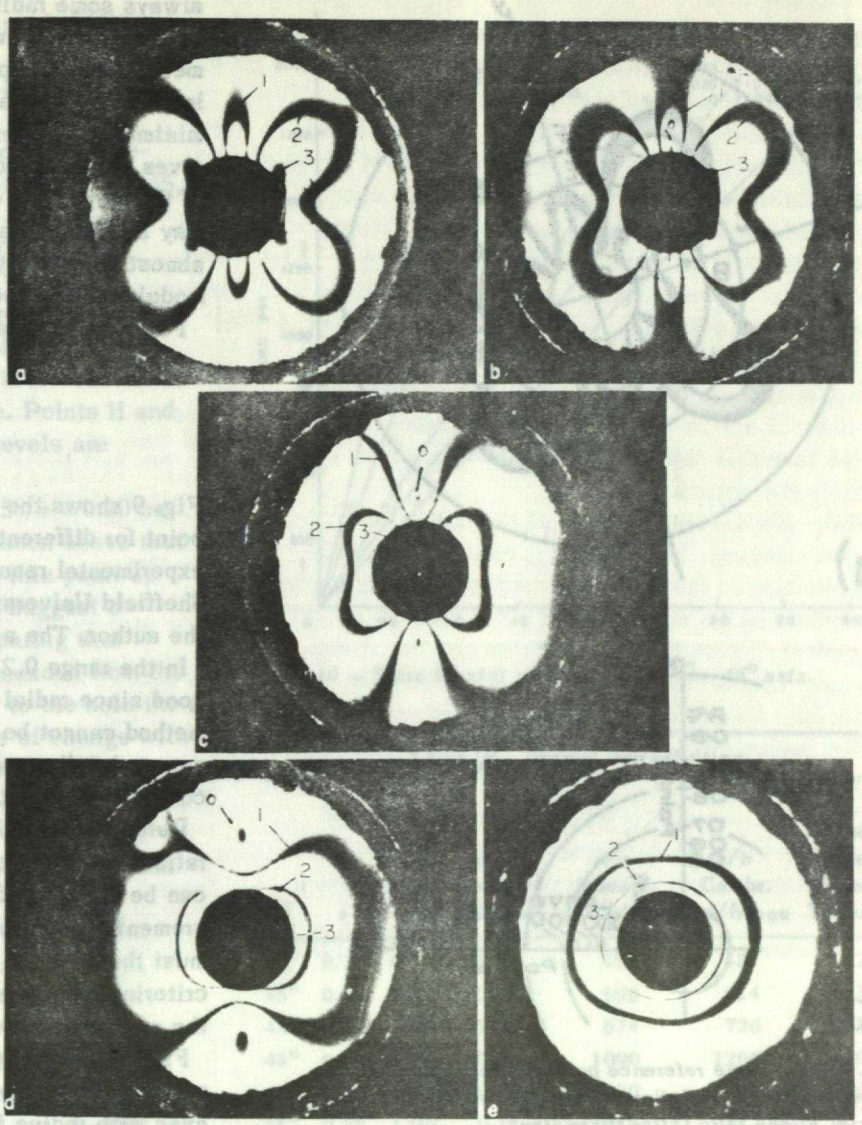

Fig. 7 – Fringe patterns under biaxial stresses: (a) 0 : 1 (b) 1 : 4 (c) 1 : 2 (d) 3 : 4 1 : 1 (after Roberts et al).[2]

pensation. This will greatly improve accuracy, but the associated viewing apparatus is considerably more expensive.

q/p FROM THE SHAPE OF THE FRINGE PATTERN – METHOD 1 – Fig. 7 shows fringe patterns for ratios of η of 0, 0.25, 0.50, 0.75 and 1. These are distinctly different patterns and therefore Roberts et al[2] proposed that the overall shape can be used to estimate the biaxial stress ratio η. Now the patterns also vary with the magnitude of p; thus, rather than rely on an observer to remember and distinguish between many patterns, it is better to compare the patterns with a standard series of photographs.

The accuracy of this method is not ideal since it is an estimate and not a measurement; this may be particularly true at low stress levels when the fringe patterns are not well developed. However, the accuracy is quite adequate for many rock mechanics problems.

q/p FROM SHAPE OF THE FRINGE PATTERN – METHOD 2 – Fig. 8a shows certain points A, B, C etc. in the meter as defined by Hiramatsu.[6] At Point H on the outer circle the fringe order is the same as that at Point X. At Point Y the fringe order is the minimum occurring in the meter.

Hiramatsu determines the ratio $1/\eta$ from the radial position of Point X or of Point Y by the relationship shown in Fig. 8b. (Note: this relationship is for a meter of diameter ratio b/a of 1/6 and not exactly for the meter used by the author and by Roberts et al in which $b/a = 1/5$.) Young's modulus and Poisson's ratio have very little effect on the position of these points.

When η is between 0 and 0.5, Point X is used for the determination whereas when η is between 0.5 and 1 Point Y is used. The radial position of Point X does not vary much as η increases so errors could be significant. This criticism does not apply to Point Y where the radial position varies rapidly in the range 0.5 to 1.

q/p BY OBSERVATION OF THE ZERO POINT ON THE $\theta = 0°$ AXIS – It can be seen from Fig. 6 that on the $\theta = 0°$ axis in the range $0.2 \leq \eta \leq 0.9$, there is

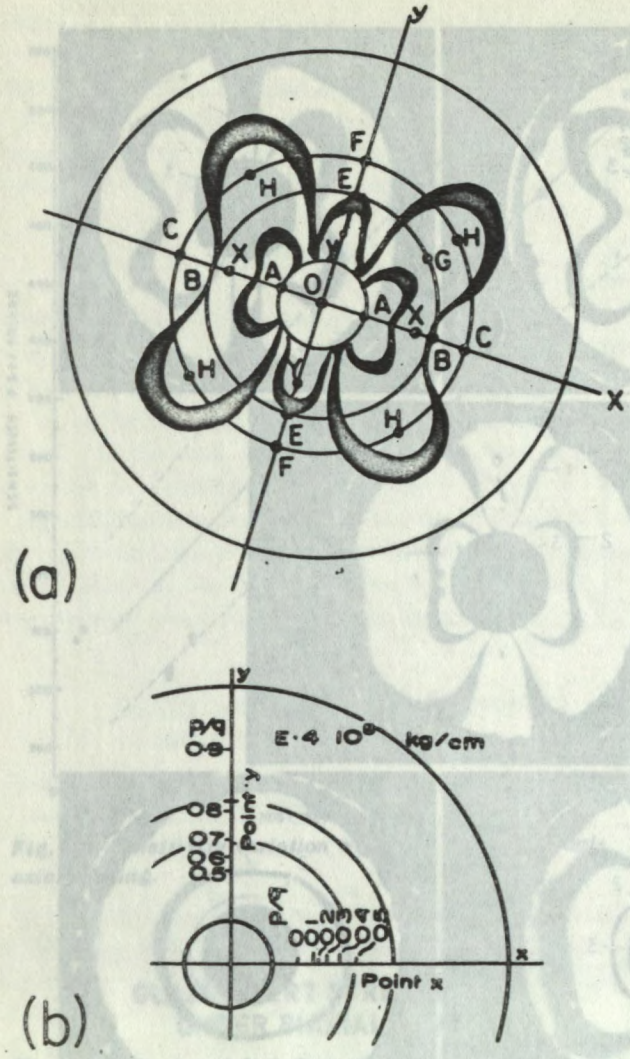

Fig. 8 – (a) Some reference points in the meter (after Hiramatsu[6]). (b) Relation between X and Y points and biaxial stress ratio (after Hiramatsu[6]).

always some radius at which the proportionality constant is zero. Thus, a black spot is seen in the meter the radial position of which varies with η i.e., in this range Hiramatsu's Y point is not merely a minimum, it is zero. Hence, observation of this point gives a measure of η that is completely independent of the magnitude of the applied stresses. Further, it may be shown that the position of this point is almost completely independent of the Young's modulus of the rock.

From Eq. 7 it can be shown that $n_x = 0$ when

$$\eta = \frac{k_2 - k_1}{k_2 + k_1}$$

Fig. 9 shows the calculated positions of the zero point for different ratios η. This figure also shows experimental results obtained by R. K. Dhir at Sheffield University using this method suggested by the author. The agreement is excellent.

In the range $0.2 \leq \eta \leq 0.35$ the accuracy will not be good since radial variation of the point is small. The method cannot be used when $0.2 > \eta > 0.9$ since the zero point disappears. However, the available range covers most practical needs.

Determination of *p* and *q*: Having determined the ratio q/p by one of the above methods, then p (or q) can be determined from a single fringe order measurement at any point. The optimum measuring point must therefore be determined for biaxial loads. The criteria for defining the optimum measuring point are the same as in the uniaxial case.

Fig. 6 shows the variation of the appropriate proportionality constants on the $\theta = 0°$, 90° and 45° axes with radius for a range of η from 0 to 1. A study

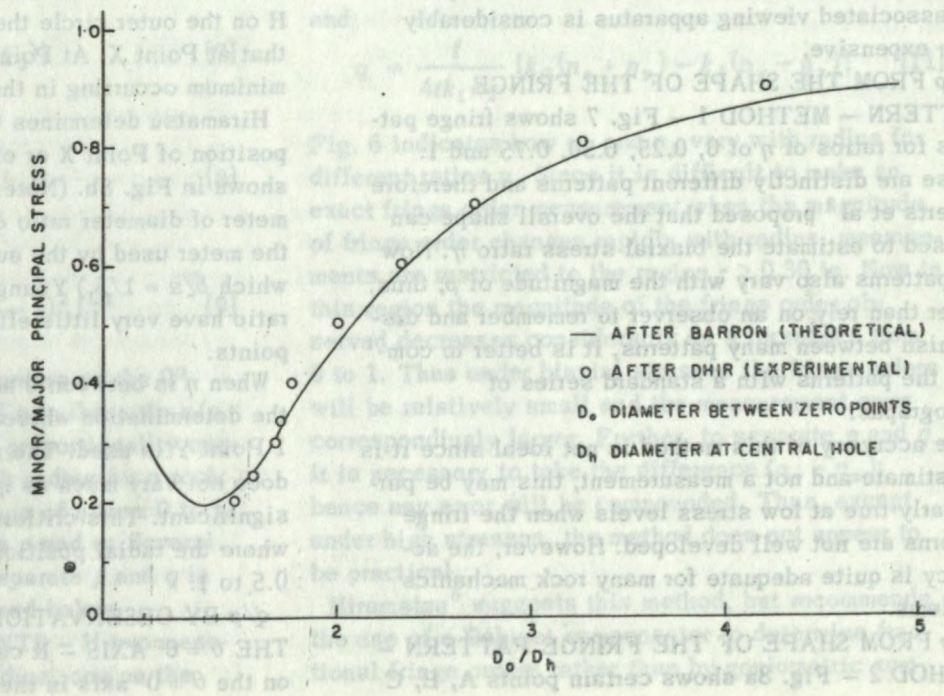

Fig. 9 – Radial variation of zero point with biaxial stress ratio.

of the graphs with the above criteria in mind showed that:

when $0 \leq \eta \leq 0.33$, measurements at a radius $r = 0.20$, $\theta = 45°$ are best.

when $0.33 \leq \eta \leq 0.9$, there is little to choose between measurements at $r = 0.35$, $\theta = 45°$ and $r = 0.35$, $\theta = 90°$.

when $\eta = 1$, all axes are the same. The region $r = 0.30$ to $r = 0.35$ is to be preferred.

Hiramatsu[6] suggests that, at low stress levels, the Point A (Fig. 8a) be used. The rate of change with radius is very large at this point and it is doubtful if an accurate measurement can be made. Points H and C that he suggests for higher stress levels are similar to those above.

Roberts et al[2] recommend that $\theta = 45°$, $r = 0.20$ be used only for uniaxial stresses. It is seen above that there is a distinct advantage in using this point up to $\eta = 0.33$. For biaxial stresses they suggest a point $r = 0.175$, $\theta = 90°$ be used. Comparing this point with the $r = 0.35$, $\theta = 90°$ recommended from the analysis above, it is seen that closer to the hole the magnitude is higher, but so is the rate of change with radius. Now, to help overcome the problem of seeing the fringe pattern accurately at this point, Roberts et al insert a collar in the central hole, which masks off the fringes to a radius of 0.175 in. Compensation is then made to the collar edge. This is a good technique. A further point in favor of the 0.175 in. radius point is that the change of sensitivity with increase of η from 0 to 1 is much less than at the $r = 0.35$ in. point.

The optimum measuring points are therefore:

when $\eta \leq 0.33$, the point is $r = 0.20$ in., $\theta = 45°$.

when $\eta \geq 0.33$, the point is $r = 0.175$ in., $\theta = 90°$ and compensation is made to the edge of the inserted collar.

Dependency on Rock Modulus: The dependency of the sensitivity on rock modulus at the optimum measuring points can now be examined for the biaxial case. As before it can be shown that, if the sensitivity is assumed independent of rock modulus, provided $E'/E > 2$ then an error greater than 20% is introduced. However, as before, this error is reduced to tolerable proportions ($< 10\%$) if the criterion is modified to $E'/E > 4$.

Laboratory Calibrations: A series of biaxial calibrations was made at various points in the meter in the aluminium block for a range of η. Some of these calibrations are shown in Fig. 10. Table II below compares the theoretical sensitivities with those obtained from the calibration curves.

The biaxial loading frame used in these experiments had insufficient capacity to enable sufficient points to be obtained to define a fair calibration when $\eta = 1$.

The results showed that:

a) The sensitivities are in reasonable agreement with theory, although the accuracy diminishes as the sensitivity diminishes.

b) The optimum measuring points theoretically determined are correct.

c) The suggestion that the zero point on the y axis be used to determine η in the range $0.2 \leq \eta \leq 0.9$ is not entirely satisfactory. The author did not obtain as clear a fringe pattern as Roberts et al (Fig. 7) and, in consequence, in one case had difficulty in seeing the zero point. This is particularly true at low stress levels when the black spot is rather diffuse. At higher stress levels and particularly in the range $\eta > 0.5$ the method worked extremely well.

d) All fringe pattems observed were symmetrical and the axis of symmetry agreed well with the applied stress directions.

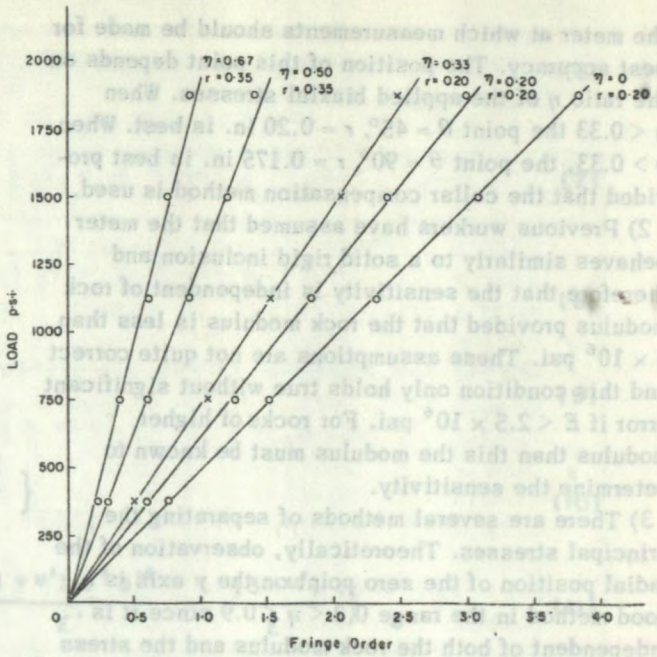

Fig. 10 – Some biaxial calibrations on $\theta = 45°$ axis.

Table II – Biaxial Sensitivities

θ	r	$=q/p$	Proportionality Constant	p/n Theory psi/fringe	p/n Calibr. psi/fringe	% Difference From Theory
45°	0.20	0.00	1.38	498	487	2.2
45°	0.20	0.20	1.15	598	614	2.7
45°	0.20	0.33	1.02	674	726	7.7
45°	0.35	0.50	0.63	1090	1260	16.0
45°	0.35	0.67	0.46	1490	1925	29.0
45°	0.35	1.00	0.26	2640	–	–

CONCLUSIONS

This study of the glass insert stressmeter has shown that:

1) There are certain optimum measuring points in

the meter at which measurements should be made for best accuracy. The position of this point depends on the ratio η of the applied biaxial stresses. When $\eta < 0.33$ the point $\theta = 45°$, $r = 0.20$ in. is best. When $\eta > 0.33$, the point $\theta = 90°$, $r = 0.175$ in. is best provided that the collar compensation method is used.

2) Previous workers have assumed that the meter behaves similarly to a solid rigid inclusion and therefore that the sensitivity is independent of rock modulus provided that the rock modulus is less than 5×10^6 psi. These assumptions are not quite correct and this condition only holds true without significant error if $E < 2.5 \times 10^6$ psi. For rocks of higher modulus than this the modulus must be known to determine the sensitivity.

3) There are several methods of separating the principal stresses. Theoretically, observation of the radial position of the zero point on the y axis is a good method in the range $0.2 < \eta < 0.9$ since it is independent of both the rock modulus and the stress magnitude. In practice this method is not always satisfactory. Comparison of the fringe pattern with a standard series of photographs would also appear to be a sound method.

4) The meter sensitivity decreases as the biaxial ratio η approaches unity; accuracy thus also decreases. Meter sensitivity can of course be increased by using a longer meter.

5) The laboratory calibrations are in relatively good agreement with theory, indicating that the meter functions correctly.

6) The axes of symmetry of the fringe pattern gave an excellent indication of applied stress directions.

Thus, it can be said that in the laboratory the meter has proved its potential. Final assessment must, of course, come from field use, but it is believed that techniques currently being developed will overcome most field problems.[7]

REFERENCES

[1] A. Roberts and I. Hawkes: The Determination of In-Situ Stress and Strain using Photoelastic Techniques, 14th colloquium Int. Soc. Rock Mechanics, Saltzburg, 1963.

[2] A. Roberts, I. Hawkes, F. T. Williams and R. K. Dhir: A Laboratory Study of the Photoelastic Stressmeter, *Int. Journal of Rock Mechanics and Mining Sciences*, vol. 1, No. 3, May 1964.

[3] M. Hetenyi: Handbook of Experimental Stress Analyses, *John Wiley and Sons*, New York, 1950.

[4] Y. Hiramatsu, Y. Niwa and Y. Oka: Measurement of Stress in the Field by Application of Photoelasticity, *Technical Report Engineering Research Institute*, Kyoto University, VIII, vol. 3, no. 37, 1957.

[5] A. Coutinho: Theory of an Experimental Method of Determining Stresses not Requiring Accurate Knowledge of the Modulus of Elasticity, *Int. Assoc. for Bridge and Structural Eng. Pub.*, vol. 7, 1949, pp. 83 to 103.

[6] Y. Hiramatsu: Measurement of Variation in Stress with a Photoelastic Stressmeter, Laboratory of Mining Engineering, Department of Mining, Kyoto University, March 1964.

[7] I. Hawkes: private communication.

Appendix I

Theoretical Analysis of Stresses in a Hollow Cylindrical Inclusion

Consider Figure 1, which shows a cross section of the hollow cylindrical inclusion in the host rock. Let the Young's modulus of the rock be E and that of the inclusion be E'. Let the Poisson's ratio of the rock and the inclusion be υ and υ' respectively. Let the outer radius of the inclusion be a and the inner radius be b. Consider any point in the test piece, (r, θ), $(a \geq r \geq b)$. Hiramatsu, Niwa and Oka (7) have shown that, when a uniaxial stress, p, is applied in the x direction, the radial, tangential and shear stresses at this point are σ_r', σ_θ' and $\tau_{r\theta}'$ respectively and are given by:

$$\sigma_r' = p\left\{2A_0 + B_0 r^{-2} - (6B_2 r^{-4} + 2C_2 + 4D_2 r^{-2})\cos 2\theta\right\} \quad (1)$$

$$\sigma_\theta' = p\left\{2A_0 - B_0 r^{-2} + (12A_2 r^2 + 6B_2 r^{-4} + 2C_2)\cos 2\theta\right\} \quad (2)$$

$$\tau_{r\theta}' = p\left\{6A_2 r^2 - 6B_2 r^{-4} + 2C_2 - 2D_2 r^{-2}\right\}\sin 2\theta \quad (3)$$

where: $$A_0 = -b^{-2} B_0/2 \quad (4)$$

$$B_0 = -\frac{a}{E}\Big/\left\{\frac{(1-\upsilon')}{E'} a b^{-2} + \frac{(1+\upsilon')}{E'} a^{-1} - \frac{(1+\upsilon)}{E}(a^{-1} - a b^{-2})\right\} \quad (5)$$

$$A_2 = -\frac{b^{-2}}{3}\left\{2C_2 + b^{-2}D_2\right\} \tag{6}$$

$$B_2 = -\frac{b^4}{3}\left\{C_2 + 2b^{-2}D_2\right\} \tag{7}$$

where: $$C_2 = \left\{\frac{\beta'\gamma - \beta\gamma'}{\alpha\beta' - \alpha'\beta}\right\} \tag{8}$$

$$D_2 = \left\{\frac{\alpha'\gamma - \gamma'\alpha}{\alpha'\beta - \alpha\beta'}\right\} \tag{9}$$

where: $$\alpha = 4(1 - a^2b^{-2})\left\{\frac{(3-\upsilon)}{E} + \frac{(1+\upsilon')}{E'}\right\} \tag{10}$$

$$\beta = 2a^{-2}\left\{\frac{(3-\upsilon)(1-a^4b^{-4})}{E} - \frac{(1+\upsilon')a^4b^{-4}}{E'} - \frac{(3-\upsilon')}{E'}\right\} \tag{11}$$

$$\gamma = -4/E \tag{12}$$

$$\alpha' = \frac{-2(1+\upsilon)(3-\upsilon)(a^{-4}b^4 - 4a^2b^{-2} + 3)}{E} + \left\{8(3+\upsilon\upsilon')a^2b^{-2} + 2(1+\upsilon')(3-\upsilon)a^{-4}b^4 - 6(1+\upsilon)(1+\upsilon')\right\}/E' \tag{13}$$

$$\beta' = \frac{-4(1+\upsilon)(3-\upsilon)(a^{-4}b^2 - a^2b^{-4})}{E} + \left\{\frac{4(3+\upsilon\upsilon')a^2b^{-4} + 4(1+\upsilon')(3-\upsilon)a^{-4}b^2 + 12(\upsilon-\upsilon')a^{-2}}{E'}\right\} \tag{14}$$

and $$\gamma' = 6(1+\upsilon)/E \tag{15}$$

Similarly, if a uniaxial stress q is applied in the y direction then the radial, tangential and shear stresses at the point (r, θ) are given by σ_r'', σ_θ'' and $\tau_{r\theta}''$ as follows:

$$\sigma_r'' = q\left\{2A_0 + B_0r^{-2} + (6B_2r^{-4} + 2C_2 + 4D_2r^{-2})\cos 2\theta\right\} \tag{16}$$

$$\sigma_\theta'' = q\left\{2A_0 - B_0r^{-2} - (12A_2r^{-4} + 6B_2r^{-4} + 2C_2)\cos 2\theta\right\} \tag{17}$$

$$\tau_{r\theta}'' = q\left\{6A_2r^2 - 6B_2r^{-4} + 2C_2 - 2D_2r^{-2}\right\}\sin 2\theta \tag{18}$$

Hence if σ_r, σ_θ and $\tau_{r\theta}$ are respectively the radial, tangential and shear stresses at the point (r, θ) under biaxial loading, then they are given by superimposing the two uniaxial solutions as follows:

$$\sigma_r = \sigma_r' + \sigma_r'' = (p+q)\left\{2A_0 + B_0r^{-2}\right\} - (p-q)\left\{6B_2r^{-4} + 2C_2 + 4D_2r^{-2}\right\}\cos 2\theta \tag{19}$$

$$\sigma_\theta = \sigma_\theta' + \sigma_\theta'' = (p+q)\left\{2A_0 - B_0r^{-2}\right\} + (p-q)\left\{12A_2r^2 + 6B_2r^{-4} + 2C_2\right\}\cos 2\theta \tag{20}$$

and $$\tau_{r\theta} = \tau_{r\theta}' - \tau_{r\theta}'' = (p-q)\left\{6A_2r^2 - 6B_2r^{-4} + 2C_2 - 2D_2r^{-2}\right\}\sin 2\theta \tag{21}$$

Now if σ_1 and σ_2 are the principal stresses at the point (r, θ), then they are given by:

$$\sigma_1 = \left\{ \frac{\sigma_r + \sigma_\theta}{2} \right\} + \tfrac{1}{2} \left\{ (\sigma_r - \sigma_\theta)^2 + 4 \tau_{r\theta}^2 \right\}^{1/2} \quad (22)$$

and

$$\sigma_2 = \left\{ \frac{\sigma_r + \sigma_\theta}{2} \right\} - \tfrac{1}{2} \left\{ (\sigma_r - \sigma_\theta)^2 + 4 \tau_{r\theta}^2 \right\}^{1/2} \quad (23)$$

Hence the principal stress difference at this point is:

$$\sigma_1 - \sigma_2 = \left\{ (\sigma_r - \sigma_\theta)^2 + 4 \tau_{r\theta}^2 \right\}^{1/2} \quad (24)$$

Now from equations (19) and (20):

$$(\sigma_r - \sigma_\theta) = 2(p+q) B_0 r^{-2} - (p-q) \left\{ 12 A_2 r^2 + 12 B_2 r^{-4} + 4 C_2 + 4 D_2 r^{-2} \right\} \cos 2\theta$$

$$= k_1 (p+q) - k_2 (p-q) \cos 2\theta \quad (25)$$

where: $k_1 = 2 B_0 r^{-2}$ (26)

and $k_2 = 4 \left\{ 3 A_2 r^2 + 3 B_2 r^{-4} + C_2 + D_2 r^{-2} \right\}$ (27)

From Equation (21)

$$2 \tau_{r\theta} = 4 (p-q) \left\{ 3 A_2 r^2 - 3 B_2 r^{-4} + C_2 - D_2 r^{-2} \right\} \sin 2\theta$$

$$= k_3 (p-q) \sin 2\theta \quad (28)$$

where $k_3 = 4 \left\{ 3 A_2 r^2 - 3 B_2 r^{-4} + C_2 - D_2 r^{-2} \right\}$ (29)

Hence, from Equations (24), (25) and (28):

$$\sigma_1 - \sigma_2 = \left\{ \left[k_1 (p+q) - k_2 (p-q) \cos 2\theta \right]^2 + k_3^2 (p-q)^2 \sin^2 2\theta \right\}^{1/2} \quad (30)$$

Consider now the fringes produced in the test piece when it is viewed by transmitted circularly polarised light. From photoelastic laws the principal stress difference, $(\sigma_1 - \sigma_2)$, at a point is directly proportional to the isochromatic fringe order, n, observed at that point and is given by:

$$n = (\sigma_1 - \sigma_2) \frac{t}{f} \quad (31)$$

where t is the thickness of the test piece and f is the optical contrast of the photoelastic material.

Thus Equations (30) and (31) define the fringe order produced at any point in the test piece when the host material is subject to biaxial stresses p and q. These equations therefore define the use of the hollow glass cylinder as a stress measuring device; a measure of the fringe order at any point is related to the applied rock stresses p and q

APPENDIX II

Table of Calculated Constants for Different Moduli E and Radii r

$E^1 = 10 \times 10^6$ psi; a = 5/8 inch; b = 1/8 inch; $\nu = \nu^i = 0.25$

E	r	k_1	k_2	k_3	$k_1 - k_2$	$k_1 + k_2$	$(k_1^2 + k_3^2)^{1/2}$
1.0×10^6	0.125	-1.5624	-3.1370	0	1.5746	-4.6994	1.5625
	0.150	-1.0850	-1.6522	-1.4752	0.5672	-2.7372	1.8314
	0.175	-0.7971	-1.1799	-1.9365	0.3828	-1.9770	2.0943
	0.200	-0.6103	-1.0418	-2.0617	0.4315	-1.6521	2.1503
	0.225	-0.4822	-1.0222	-2.0667	0.5600	-1.5044	2.1224
	0.250	-0.3905	-1.0442	-2.0285	0.6537	-1.4347	2.0659
	0.275	-0.3227	-1.0783	-1.9764	0.7556	-1.4010	2.0027
	0.300	-0.2712	-1.1132	-1.9219	0.8420	-1.3844	1.9410
	0.325	-0.2310	-1.1444	-1.8693	0.9134	-1.3754	1.8836
	0.350	-0.1992	-1.1705	-1.8200	0.9713	-1.3697	1.8310
	0.375	-0.1735	-1.1913	-1.7744	1.0178	-1.3648	1.7830
	0.500	-0.0976	-1.2296	-1.5863	1.1320	-1.3272	1.5894
	0.625	-0.0624	-1.1933	-1.4300	1.1309	-1.2557	1.4315
2.5×10^6	0.125	-1.4285	-2.8343	0	1.4058	-4.2628	1.4286
	0.150	-0.9920	-1.4950	-1.3337	0.5030	-2.4870	1.6623
	0.175	-0.7288	-1.0701	-1.7520	0.3413	-1.7989	1.8977
	0.200	-0.5579	-0.9473	-1.8672	0.3894	-1.5052	1.9489
	0.225	-0.4408	-0.9318	-1.8741	0.4910	-1.3726	1.9254
	0.250	-0.3570	-0.9540	-1.8422	0.5970	-1.3110	1.8766
	0.275	-0.2951	-0.9876	-1.7980	0.6925	-1.2827	1.8221
	0.300	-0.2479	-1.0221	-1.7518	0.7742	-1.2700	1.7694
	0.325	-0.2112	-1.0536	-1.7077	0.8424	-1.2648	1.7208
	0.350	-0.1821	-1.0807	-1.6669	0.8986	-1.2628	1.6769
	0.375	-0.1586	-1.1034	-1.6295	0.9448	-1.2620	1.6373
	0.500	-0.0892	-1.1612	-1.4830	1.0720	-1.2604	1.4858
	0.625	-0.0572	-1.1583	-1.3719	1.1013	-1.2153	1.3732
5.0×10^6	0.125	-1.2499	-2.4731	0	1.2332	-3.7230	1.2500
	0.150	-0.8680	-1.3063	-1.1643	0.4383	-2.1743	1.4524
	0.175	-0.6377	-0.9371	-1.5307	0.2994	-1.5748	1.6583
	0.200	-0.4882	-0.8316	-1.6329	0.3434	-1.3198	1.7045
	0.225	-0.3857	-0.8199	-1.6409	0.4342	-1.2056	1.6858
	0.250	-0.3124	-0.8414	-1.6153	0.5290	-1.1538	1.6453
	0.275	-0.2582	-0.8730	-1.5791	0.6148	-1.1312	1.6002
	0.300	-0.2169	-0.9056	-1.5415	0.6887	-1.1225	1.5568
	0.325	-0.1848	-0.9358	-1.5059	0.7510	-1.1206	1.5173
	0.350	-0.1593	-0.9625	-1.4733	0.8032	-1.1218	1.4820
	0.375	-0.1388	-0.9855	-1.4440	0.8467	-1.1243	1.4508
	0.500	-0.0780	-1.0555	-1.3360	0.9775	-1.1335	1.3384
	0.625	-0.0499	-1.0782	-1.2644	1.0393	-1.1281	1.2655
10.0×10^6	0.125	-1.0	-2.0	0	1.0	-3.0	1.0
	0.150	-0.6943	-1.0578	-0.9420	0.3635	-1.7521	1.1704
	0.175	-0.5101	-0.7604	-1.2394	0.2503	-1.2705	1.3404
	0.200	-0.3905	-0.6764	-1.3234	0.2859	-1.0669	1.3799
	0.225	-0.3085	-0.6684	-1.3314	0.3599	-0.9769	1.3668
	0.250	-0.2499	-0.6874	-1.3124	0.4375	-0.9373	1.3361
	0.275	-0.2065	-0.7147	-1.2851	0.5082	-0.9212	1.3017
	0.300	-0.1735	-0.7431	-1.2567	0.5696	-0.9166	1.2687
	0.325	-0.1478	-0.7697	-1.2301	0.6219	-0.9175	1.2391
	0.350	-0.1275	-0.7936	-1.2062	0.6661	-0.9211	1.2130
	0.375	-0.1110	-0.8147	-1.1851	0.7037	-0.9257	1.1904
	0.500	-0.0624	-0.8866	-1.1132	0.8242	-0.9490	1.1150
	0.625	-0.0399	-0.9247	-1.0751	0.8848	-0.9656	1.0759

DISCUSSION

GLASS INSERT STRESSMETER

by K. Barron

AIME Transactions, 1965, vol. 235, p. 000.

I. Hawkes *(Postgraduate School in Mining, University of Sheffield, Sheffield, England)* – The photoelastic stressmeter is proving to be a very practical tool for 'in-situ' measurements in the fields of civil and mining engineering and Barron's article has therefore come at a very opportune time, supplementing as it does, the considerable amount of laboratory and field data which is being accumulated.[1,2,3] There are however several points relating the application of Barron's conclusions to the practical use of the meter which require further elucidation.

EASE OF READING

If the photoelastic stressmeter is to have a wide application, the fringe orders must be easily measured. The system adopted by the writer and his colleagues at Sheffield for the uniaxial stress case is to read the fringe order at the 45° point, 0.20 in. from the center (1¼ in. diam meter). This procedure has been recommended because the fringes not at this point form a very distinct 'eye' which is obvious even to those who have had little experience with photoelastic fringe patterns. Barron points out that this point can also be used up to a stress ratio of 0.33 and in practice this is normally done.

In biaxial fields above a ratio of 0.33 the 'eye' is no longer apparent and the fringe order must be ascertained at some other point. The writer and his colleagues experimented at various points and finally chose a point at a distance 0.175 in. (1¼ in. diam meter) on the minor stress axis and fixed this point on the meter by inserting a collar of this diameter.

This procedure enables the 'eye' technique to be used for uniaxial stresses as the 'eye' falls outside the collar; any other technique for biaxial patterns would require lines to be engraved on the meter itself and reading difficulties would be experienced by all but the most highly trained.

It is interesting to point out that in a great many field applications ranging from underground pillars to building foundation piles the stresses measured have been uniaxial. In such cases, reading the fringe order has been simple even for unskilled persons.

SENSITIVITY

The photoelastic stressmeter acts as an inclusion, and as such its theoretical behavior is as described by Barron's mathematical analysis. When considering its practical application, however, it must be remembered that rocks and concrete are not mathematically ideal substances. The theory relates the fringe order in the meter to the stresses and the E (Young's Modulus) and the μ (Poisson's Ratio) values of the surrounding material. There is of course no unique E or μ value for rocks or concrete. These values change both with stress level and time load application sometimes to the order of 300%. We at Sheffield have very accurately calibrated the photoelastic stressmeter in a wide range of materials and have also measured the average E values for these materials. The results prove that the meter sensitivity

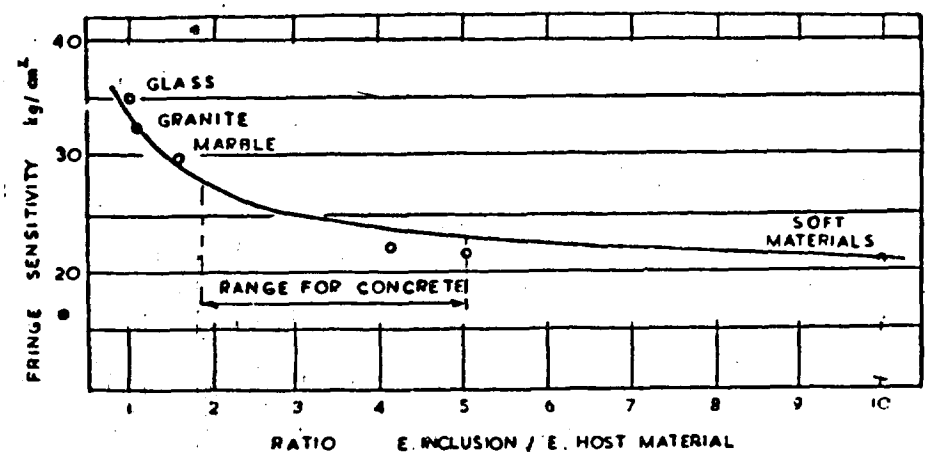

Fig. 1

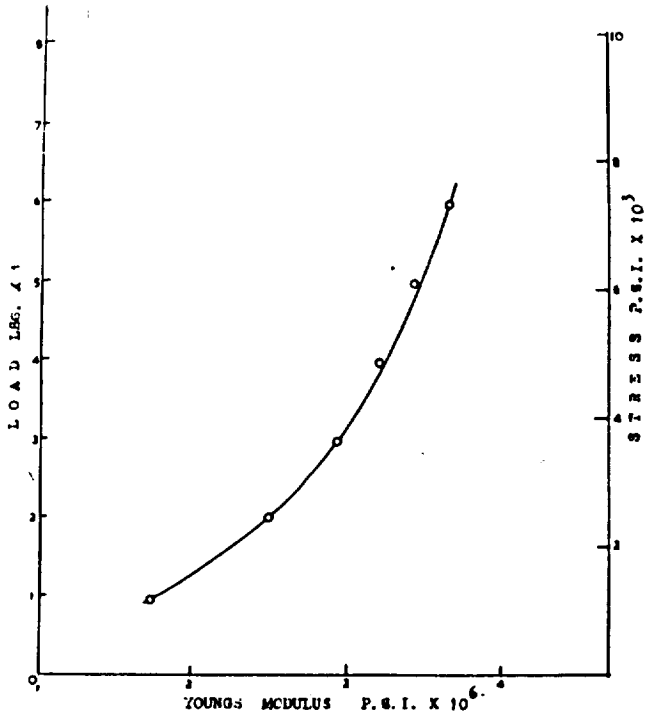

Fig. 2 — Variation of Young's modulus with stress for Darley Dale sandstone.

is in fact independent of the E value of the rock when the average E value is less than 5×10^6 psi. The correlation between these results and those obtained theoretically by Barron are illustrated in Fig. 1. Materials with an average modulus greater than 7×10^6 psi behave in a reasonably elastic manner and the results from such materials conform very well with theory. Materials with an E value below 5×10^6 psi however usually behave in a complete non-elastic manner and their E values vary to a large extent with stress level. Fig. 2 gives a typical result for a very homogeneous rock, Darley Dale Sandstone, in which the E value changes from 1.5×10^6 to 3.8×10^6 psi over a stress range of 600 to 6000 psi.

The E value of this rock is quoted at 4×10^6 psi and when the photoelastic stressmeter is inserted into it, the meter behaves as a rigid inclusion.

Barron points out in his article, and it cannot be too strongly emphasized, that the use of the meter is not limited to weak rocks. In strong rocks, the sensitivity is a function of the E value but in such materials the E value can be ascertained with sufficient accuracy and the advantage of being a biaxial gauge coupled with its basic simplicity and cheapness render it a tool of almost universal application in the field of stress analysis.

REFERENCES

[1] A. Roberts, I. Hawkes and F. T. Williams: Some Field Applications of the Photoelastic Stressmeter, *Int. J. Rock Mech. and Min. Sciences*, 1965, vol. 1, No. 4.

[2] A. Roberts: The Photoelastic Glass Insertion Stress Meter, presented to *Groupement pour l'Avancement des Methodes d'Analyse des Constraintes*, Paris, December 1964.

[3] I. Hawkes, R. K. Dhir and H. Rose: An Application of Photoelastic Transducers to Load Measurement in Building Foundations, *Civil Engineering*, December 1964.

K. Barron *(Author's Reply)* — I agree entirely with Dr. Hawkes when he emphasizes the fact that the fringe pattern must be easily interpreted. His technique for measuring the fringe order in the meter satisfies this requirement. However, the greatest problem in interpretation of the fringe patterns by unskilled workers is, I believe, not that of measuring the fringe order but that of determining the biaxial stress ratio. I believe that in this content the "zero point" method, where applicable, adds considerably to the ease of fringe pattern interpretation.

Whether or not in practice it is safe to consider the meter sensitivity as being independent of host rock modulus when this modulus is as high as 5×10^6 psi depends on the accuracy required in the experiment. As is shown in the paper, a 20% error can be introduced by this assumption, however, I concede that in many rock mechanics problems this is not necessarily a significant error. I am of the opinion that the experimenter should at least be aware that he is introducing such an error in the results.

As Dr. Hawkes illustrates in his Fig. 2, many rocks do not have a linear stress-strain relationship and therefore there is some doubt as to which modulus should be used. For accurate measurement the tangent modulus at the particular stress level in the rock should be used. If deemed necessary, this could be achieved in the following manner. First determine the stress-strain relationship of the rock, (as Dr. Hawkes Fig. 2). From this curve select or guess some modulus for the rock and using this value interpret the fringes in the meter to determine the stress level. Using this stress level, determine the tangent modulus from the stress-strain curve of the rock. Use this modified modulus, reinterpret the fringe pattern to give a modified stress level. Continuation of this procedure of successive approximations should result in a rapid convergence which will yield both the correct modulus and the correct stress level.